AMERICAN SOCIETY FOR MICROBIOLOGY | Applied and Environmental Microbiology®

GENETICS AND MOLECULAR BIOLOGY

RifZ (AMED_0655) Is a Pathway-Specific Regulator for Rifamycin Biosynthesis in *Amycolatopsis mediterranei*

Chen Li,[a] Xinqiang Liu,[b,c] Chao Lei,[c] Han Yan,[c] Zhihui Shao,[c] Ying Wang,[a] Guoping Zhao,[a,c,d] Jin Wang,[c] Xiaoming Ding[a]

State Key Laboratory of Genetic Engineering, Department of Microbiology and Microbial Engineering, School of Life Sciences, Fudan University, Shanghai, China[a]; University of Chinese Academy of Sciences, Beijing, China[b]; CAS Key Laboratory of Synthetic Biology, Institute of Plant Physiology and Ecology, Shanghai Institutes for Biological Sciences, Chinese Academy of Sciences, Shanghai, China[c]; Department of Microbiology and Li Ka Shing Institute of Health Sciences, The Chinese University of Hong Kong, Prince of Wales Hospital, Shatin, New Territories, Hong Kong SAR, China[d]

ABSTRACT Rifamycin and its derivatives are particularly effective against the pathogenic mycobacteria *Mycobacterium tuberculosis* and *Mycobacterium leprae*. Although the biosynthetic pathway of rifamycin has been extensively studied in *Amycolatopsis mediterranei*, little is known about the regulation in rifamycin biosynthesis. Here, an *in vivo* transposon system was employed to identify genes involved in the regulation of rifamycin production in *A. mediterranei* U32. In total, nine rifamycin-deficient mutants were isolated, among which three mutants had the transposon inserted in *AMED_0655* (*rifZ*, encoding a LuxR family regulator). The *rifZ* gene was further knocked out via homologous recombination, and the transcription of genes in the rifamycin biosynthetic gene cluster (*rif* cluster) was remarkably reduced in the *rifZ* null mutant. Based on the cotranscription assay results, genes within the *rif* cluster were grouped into 10 operons, sharing six promoter regions. By use of electrophoretic mobility shift assay and DNase I footprinting assay, RifZ was proved to specially bind to all six promoter regions, which was consistent with the fact that RifZ regulated the transcription of the whole *rif* cluster. The binding consensus sequence was further characterized through alignment using the RifZ-protected DNA sequences. By use of bionformatic analysis, another five promoters containing the RifZ box (CTACC-N8-GGATG) were identified, among which the binding of RifZ to the promoter regions of both *rifK* and *orf18* (*AMED_0645*) was further verified. As RifZ directly regulates the transcription of all operons within the *rif* cluster, we propose that RifZ is a pathway-specific regulator for the *rif* cluster.

IMPORTANCE To this day, rifamycin and its derivatives are still the first-line antituberculosis drugs. The biosynthesis of rifamycin has been extensively studied, and most biosynthetic processes have been characterized. However, little is known about the regulation of the transcription of the rifamycin biosynthetic gene cluster (*rif* cluster), and no regulator has been characterized. Through the employment of transposon screening, we here characterized a LuxR family regulator, RifZ, as a direct transcriptional activator for the *rif* cluster. As RifZ directly regulates the transcription of the entire *rif* cluster, it is considered a pathway-specific regulator for rifamycin biosynthesis. Therefore, as the first regulator characterized for direct regulation of *rif* cluster transcription, RifZ may provide a new clue for further engineering of high-yield industrial strains.

KEYWORDS *Amycolatopsis mediterranei*, rifamycin, rif, RifZ, pathway-specific regulator

Received 28 November 2016 **Accepted** 26 January 2017

Accepted manuscript posted online 3 February 2017

Citation Li C, Liu X, Lei C, Yan H, Shao Z, Wang Y, Zhao G, Wang J, Ding X. 2017. RifZ (AMED_0655) is a pathway-specific regulator for rifamycin biosynthesis in *Amycolatopsis mediterranei*. Appl Environ Microbiol 83: e03201-16. https://doi.org/10.1128/AEM.03201-16.

Editor Shuang-Jiang Liu, Chinese Academy of Sciences

Address correspondence to Jin Wang, wangj01@hotmail.com, or Xiaoming Ding, xmding74@fudan.edu.cn.

C. Li and X. Liu are co-first authors.

Amycolatopsis mediterranei is well known to produce the commercially important ansamycin antibiotic rifamycin, whose derivatives are particularly effective against pathogenic mycobacteria (1). These years, with the emergence of multidrug-resistant (MDR) and totally drug-resistant (TDR) tuberculosis (2, 3), an in-depth study of rifamycin biosynthesis and the development of new effective derivatives become more and more urgent. Due to their ability to tightly bind to prokaryotic RNA polymerases, rifamycins kill bacteria by blocking the transcription elongation (4, 5). In the past 2 decades, most processes in rifamycin biosynthesis have been characterized, and the nearly 90-kb rifamycin biosynthetic gene cluster (*rif* cluster) from several *A. mediterranei* strains has been sequenced (6–9); it starts with *AMED_0613* (*rifS*) and ends with *AMED_0655* (the last gene in the *rif* cluster, thus named *rifZ*) in *A. mediterranei* U32 (Fig. 1). The cluster includes genes involved in 3-amino-5-hydroxybenzoic acid (AHBA) biosynthesis (*rifG-rifN* operon and *rifJ*), polyketide biosynthesis (*rifA-rifE* operon), and rifamycin modification and export (6, 10–14). Although two *rif* genes are annotated as regulatory genes (Fig. 1), little is known about the regulation of rifamycin biosynthesis (9).

Secondary metabolisms can be regulated by either global regulators or pathway-specific regulators. In actinobacteria, GlnR and PhoP are two key global regulators that govern the nitrogen and phosphate metabolisms and then affect the biosynthesis of the secondary metabolites (15–19). In addition, the pathway-specific regulators are also important for the regulation of the biosynthesis of secondary metabolites. The large ATP-binding regulators of the LuxR family (LAL regulators) constitute a large family of pathway-specific regulators, and many regulators in this family have been identified in actinobacteria, such as AveR (20), PikD (21), RapH (22), GdmRI and GdmRII (23, 24), SlnR (25), Dbv3 (26), and Tei16* (27). However, as no LuxI proteins have been found in actinobacteria and no N-acyl-L-homoserine lactone (AHL)-sensing system has been reported for Gram-positive bacteria, LuxR family regulators in actinobacteria are unlikely to be controlled by quorum-sensing signals similar to those in *Vibrio fischeri* (28).

In *A. mediterranei* U32, the biosynthesis of rifamycin was influenced after deletion of *glnR* (29). However, as GlnR is unable to bind the promoter region of the *AMED_0615* operon (our unpublished data), the regulation must be conducted via an indirect way. Meanwhile, no pathway-specific regulators have ever been reported for the *rif* cluster. Therefore, to identify novel regulators for *rif* transcription, a transposon mutagenesis library was constructed in *A. mediterranei* U32 and a pathway-specific regulator for the *rif* cluster was identified and further characterized in this study.

RESULTS AND DISCUSSION

Screening of Tn*316* transposon mutants defective in rifamycin production. An efficient transposon system of Tn*316* derived from *Nocardia asteroides* YP21 (30, 31) was applied to generate a transposon mutant library in *A. mediterranei* U32 with the efficiency of 1.12×10^2 CFU per microgram Tn*316*. Tn*316* integration sites were determined via plasmid rescue experiments followed by DNA sequencing and were found to be randomly distributed on the U32 chromosome. Based on our previous studies, this transposon system also works efficiently in *Streptomyces* (32, 33), which therefore suggests that this *in vivo* transposon system may also be applied in functional genomics study of other actinomycetes.

A library of 20,000 transposon mutants was constructed to screen mutants defective in rifamycin production (see Materials and Methods). In total, 11 mutants defective in rifamycin production were obtained, and 9 of them had the transposon inserted within the *rif* cluster, including the AHBA formation genes (mutant no. 115C07), polyketide biosynthesis genes (no. 039F10, no. 112C08, no. 110H05, and no. 023A12), a P450 enzyme gene, *AMED_0616* (no. 050D05), and a regulatory gene, *rifZ* (no. 061H02, no. 063H06, and no. 063H07) (Fig. 1 and Table 1).

Among these mutants, the one with a mutation in *rifZ*, which encodes a LuxR family regulator and is located at the end of the *rif* cluster (9, 14), drew our attention. Bioinformatics analysis revealed a helix-turn-helix (HTH) LuxR-type DNA binding motif in the C terminus of RifZ (see Fig. S2 in the supplemental material). However, no

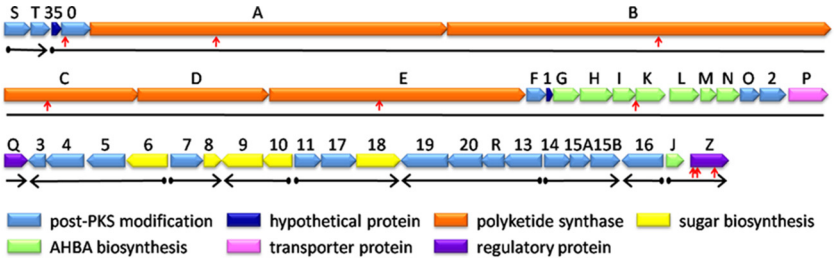

FIG 1 Schematic chart of the *rif* cluster in *A. mediterranei* U32. The transposon insertional sites listed in Table 1 are labeled with vertical red arrows. The length and direction of the 10 operons in the *rif* cluster are indicated by solid horizontal black arrows. Genes listed: S, *rifS*; T, *rifT*; 35, *orf35* (*AMED_0615*); 0, *orf0* (*AMED_0616*); A, *rifA*; B, *rifB*; C, *rifC*; D, *rifD*; E, *rifE*; F, *rifF*; 1, *orf1* (*AMED_0623*); G, *rifG*; H, *rifH*; I, *rifI*; K, *rifK*; L, *rifL*; M, *rifM*; N, *rifN*; O, *rifO*; 2, *orf2* (*AMED_0632*); P, *rifP*; Q, *rifQ*; 3, *orf3* (*AMED_*0635); 4, *orf4* (*AMED_0636*); 5, *orf5* (*AMED_0637*); 6, *orf6* (*AMED_0638*); 7, *orf7* (*AMED_0639*); 8, *orf8* (*AMED_0640*); 9, *orf9* (*AMED_0641*); 10, *orf10* (*AMED_0642*); 11, *orf11* (*AMED_0643*); 17, *orf17* (*AMED_0644*); 18, *orf18* (*AMED_0645*); 19, *orf19* (*AMED_0646*); 20, *orf20* (*AMED_0647*); R, *rifR*; 13, *orf13* (*AMED_0649*); 14, *orf14* (*AMED_0650*); 15A, *orf15A* (*AMED_0651*); 15B, *orf15B* (*AMED_0652*); 16, *orf16* (*AMED_0653*); J, *rifJ*; Z, *rifZ* (*AMED_0655*).

autoinducer binding domain was identified, which indicated that the regulation of RifZ was different from the typical quorum-sensing model in Gram-negative bacteria (e.g., *V. fischeri*).

RifZ activates the transcription of *rif* genes in *A. mediterranei* U32. The *rifZ* gene was further knocked out via homologous recombination to fully uncover its function in *A. mediterranei* U32. First of all, the deletion of *rifZ* did not affect bacterial growth either on the plate (Fig. 2A) or in the liquid culture (Fig. 2B), which indicated that *rifZ* was not related to the cell's growth. What is more, it was noteworthy that there was different pigmentation of the *rifZ* knockout mutant (KO) and of NC (KO strain integrated with pDZL803, a negative control) with respect to the wild-type strain (WT) and to C (KO strain integrated with pDZL8031, a complementation strain) when growing on the plate. And this may be caused by their different capability for rifamycin biosynthesis, because rifamycins usually appeared golden on the plate. So, the yield of rifamycins was then detected by both the bacterial inhibition test (Fig. 2C) and the chemical method (Fig. 2D), which showed that the KO's yield of rifamycins dropped significantly, just as in the transposon-deactivated *rifZ* mutants, and subsequent complementation of *rifZ* with its intact promoter restored the rifamycin production to a level comparable to that of the wild type (Fig. 2C and D). All the above-described results illustrated in Fig. 2 indicated that RifZ positively regulated the biosynthesis of rifamycin.

A reverse transcription (RT)-PCR assay was then employed to determine whether RifZ regulated the transcription of the *rif* cluster. Total RNA was extracted from the wild-type strain, the *rifZ* knockout mutant, the complementation strain integrated with pDZL8031, and the mutant integrated with the control plasmid pDZL803. The RT-PCR results showed that the levels of transcription of *orf2* (*AMED_0632*) and *rifP* were very low and even undetectable in the wild type, which was possibly caused by their

TABLE 1 Tn*316* insertional locations in *A. mediterranei* U32

Transposon mutant no.	Tn*316* insertional site (bp)	Inactivated gene	Within *rif* cluster?
050D05	628514 to 628513	*AMED_0616*	Yes
039F10	634881 to 634882	*rifA*	Yes
112C08	635269 to 635270	*rifB*	Yes
110H05	660734 to 660735	*rifC*	Yes
023A12	673636 to 673537	*rifE*	Yes
115C07	684168 to 684167	*rifK*	Yes
061H02	716703 to 716704	*rifZ*	Yes
063H06	715689 to 715690	*rifZ*	Yes
063H07	715720 to 715721	*rifZ*	Yes
109A12	2462543 to 2462542	*AMED_2309*	No
050F04	5030598 to 5030597	*AMED_4574*	No

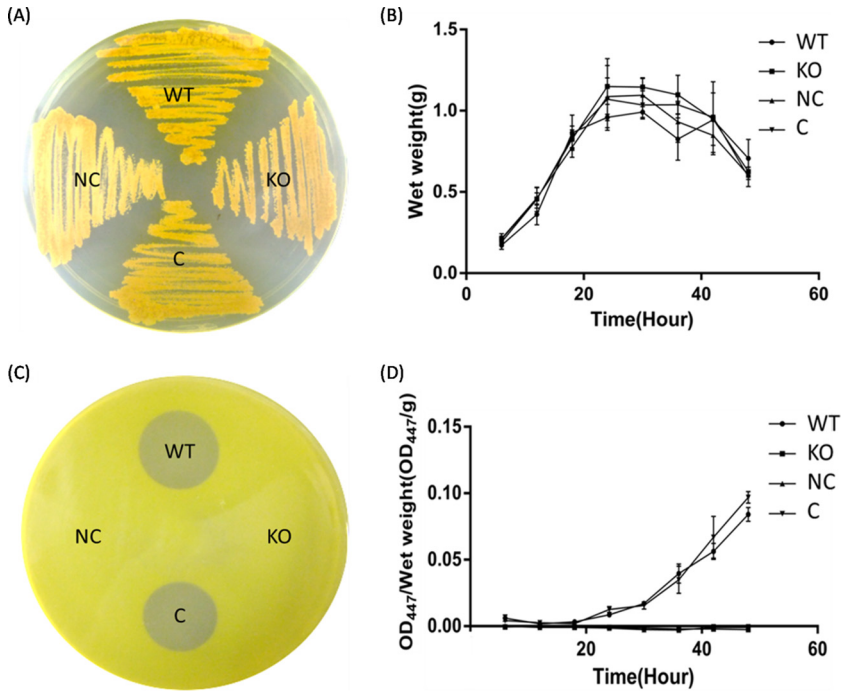

FIG 2 RifZ stringently regulates rifamycin biosynthesis in *A. mediterranei* U32. (A) Growth of *A. mediterranei* strains on a Bennet plate. (B) Growth curves of different *A. mediterranei* strains. (C) Bacterial inhibition test of different *A. mediterranei* strains using *Sarcina lutea* as the indicator. (D) Rifamycin production by different *A. mediterranei* strains, detected by a chemical method. Both NC and KO strains lost the ability to produce rifamycin. WT, wild type; KO, *rifZ* knockout mutant; NC, KO strain integrated with pDZL803, a negative control; C, KO strain integrated with pDZL8031, a complementation strain.

physical location within the cluster, i.e., near the end of a large operon, or by the independent regulation of unknown factors. Except for these two genes, the transcription of all other genes significantly decreased in the null mutant and the null mutant with the control plasmid, while their transcription was recovered in the complementation strain (Fig. 3). Based on these results, one might conclude that RifZ is a positive regulator for the transcription of the *rif* cluster.

RifZ is a pathway-specific regulator for the *rif* cluster. To determine whether RifZ was able to directly bind to the promoter regions of its target genes in the *rif* cluster, overexpression of RifZ was performed in *Escherichia coli*. However, although different expression conditions that employed different plasmids with distinct promoters and different *E. coli* hosts were tried, RifZ either failed to be expressed or remained in the form of an insoluble inclusion body. Renaturation of the inclusion body was also attempted but failed (data not shown). We then resorted to overexpressing truncated forms of RifZ that contained the DNA binding domain (amino acids [aa] 346 to 398). Distinct truncated RifZs were tested, and only RifZ-5, which contained the sequence of aa 320 to 404, was soluble in *E. coli* hosts under the tested conditions (see Fig. S3 and S4 in the supplemental material).

Meanwhile, the cotranscription of *rif* cluster genes in *A. mediterranei* U32 was examined by RT-PCR analysis, which indicated that the *rif* cluster was divided into 10 operons transcriptionally, sharing six promoter regions (Fig. 1; see also Fig. S5 in the supplemental material). Then, all the promoter regions were prepared as 6-carboxyfluorescein (FAM)-labeled probes and were used for electrophoretic mobility shift assay (EMSA) with purified RifZ-5. For those four promoters of divergent operons (promoters of *orf6* and *orf7*, *orf10* and *orf11*, *orf13* and *orf14*, and *orf16* and *rifJ* [Fig. 1]), relatively long probes covering whole intergenic regions were prepared for each promoter region. According to the EMSA results, we found that all these six probes could be specifically bound by RifZ-5 (see Fig. S6A in the supplemental

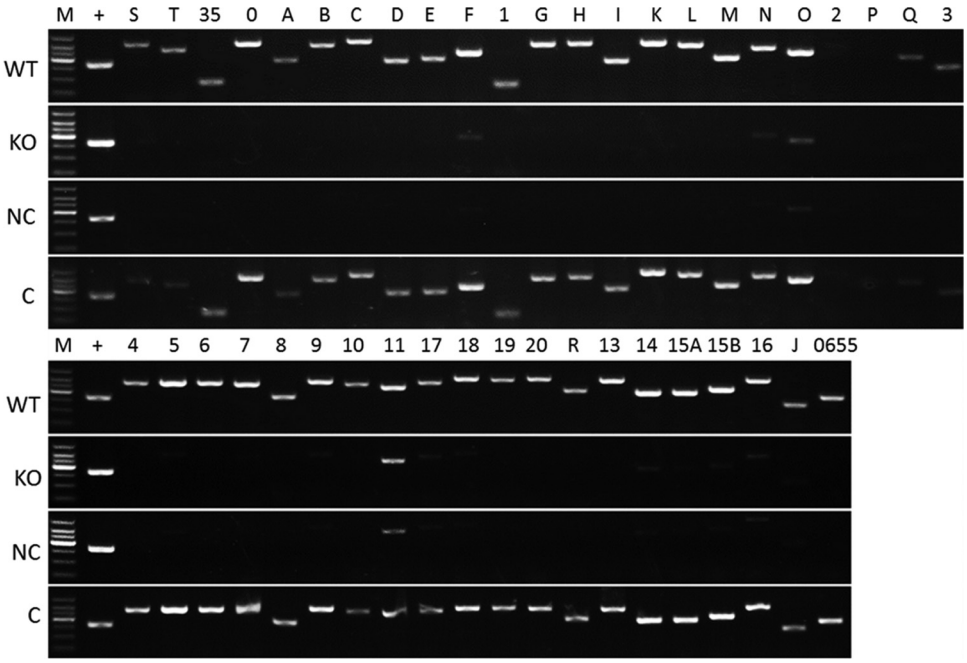

FIG 3 RT-PCR analysis of the transcription of genes in the *rif* cluster in different *A. mediterranei* strains. No PCR bands were observed when total RNA without reverse transcription was employed as the template, which indicated that the RNA samples were not contaminated by genomic DNA (data not shown). WT, wild type; KO, *rifZ* knockout mutant; NC, KO strain integrated with pDZL803, a negative control; C, KO strain integrated with pDZL8031, a complementation strain; M, DL1000 DNA ladder; +, the *rpoB* gene, used as an internal control. The analyzed genes were in the same order as shown in Fig. 1, where "S" stood for *rifS*, 35 stood for *orf35*, etc.

material), which could well explain the RifZ-mediated transcriptional regulation of most genes in the *rif* cluster. A DNase I footprinting experiment was further employed to determine the RifZ-5 binding sequences in the above-mentioned promoter regions (Fig. 4A; see also Fig. S7 in the supplemental material). Then, a consensus DNA sequence of CTACC-N8-GGATG (RifZ box), which was composed of a pair of imperfect inverted repeats, was identified through DNA alignment analysis (Fig. 4B). As revealed by the DNase I footprinting results, the binding affinity of RifZ-5 to promoter regions of *orf35* (*AMED_0615*) and *rifS* was the strongest, where 2 μg RifZ-5 could provide obvious protection of target DNA sequences against DNase I digestion, while the binding affinity to the others was relatively weaker, i.e., *orf6* (*AMED_0638*), *orf11* (*AMED_0643*), *orf14* (*AMED_0650*), and *orf16* (*AMED_0653*).

Moreover, the binding motif was used to search for the promoter regions throughout the genome of U32, and five new promoter regions containing the RifZ box were identified (see Table S2 in the supplemental material), among which were *rifK* and *orf18* (*AMED_0645*), located within the *rif* cluster. RifK is an AHBA synthase and plays an important role in the AHBA biosynthesis, while Orf18 is a nucleotide diphosphate (NDP)-hexose 2,3-dehydratase and takes part in sugar biosynthesis (9). As both genes transcribed from their operons' promoters and no promoter regions had been previously predicted, the transcriptome data of *A. mediterranei* U32 (34) were then reanalyzed. Both *rifK* and *orf18* (*AMED_0645*) were found to transcribe at an obviously higher level than their previous genes (see Fig. S8 in the supplemental material), indicating that both genes might transcribe from their own promoters in addition to their operons' promoters. Both promoter regions of *rifK* and *orf18* were then selected to verify the accuracy of the bioinformatics prediction, and further EMSA (Fig. S6B) and DNase I footprinting (Fig. 5) confirmed the specific binding of RifZ-5 to the promoter regions of *rifK* and *orf18*, respectively. As RifZ directly activated the majority of *rif* genes, it was considered a pathway-specific regulator for the transcription of the *rif* cluster.

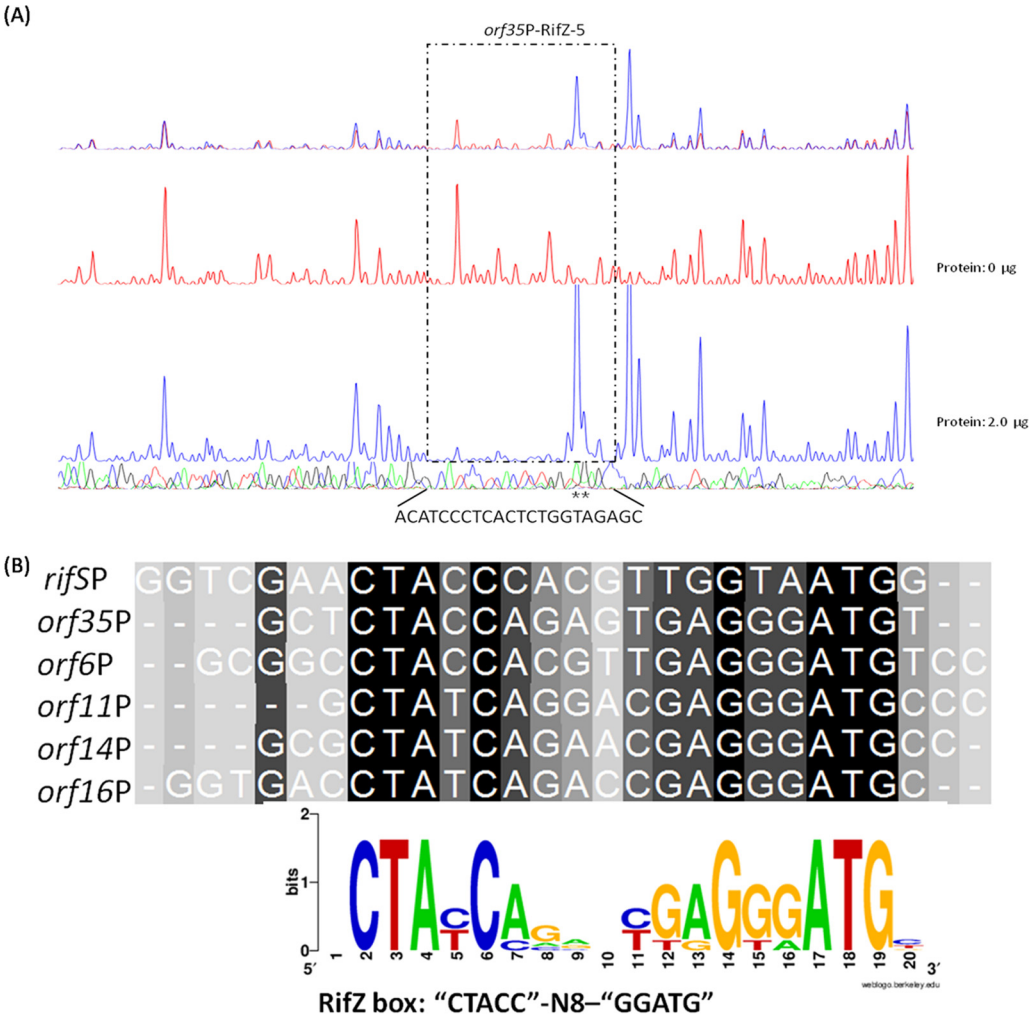

FIG 4 Characterization of the RifZ-5-protected DNA sequences by DNase I footprinting assay and the speculative RifZ box. (A) Analysis of the RifZ-5-protected DNA sequences in the promoter region of *orf35* by DNase I footprinting assay. The electrophoretograms of the control reaction (without RifZ-5, red line) and experimental reaction (with RifZ-5, blue line) are shown in the upper panel, and the lower panel shows the DNA sequencing results. Precise DNA sequences protected by RifZ-5 are indicated at the bottom, and hypersensitive sites are indicated with asterisks. The results of RifZ-5-protected DNA sequences in the promoter regions of other target genes, including *rifS*, *orf6*, *orf11*, *orf14*, and *orf16*, are shown in Fig. S7 in the supplemental material. (B) The RifZ binding consensus sequence of CTACC-N8-GGATG was obtained through alignment using the RifZ-5-protected DNA sequences in the promoter regions of all six target genes. The sequence logo at the bottom was generated by web-based WebLogo (version 2.8.2).

MATERIALS AND METHODS

Bacterial strains, media, and primers. Methylation-deficient *Escherichia coli* JM110 was used to propagate plasmid Tn*316*. *A. mediterranei* U32 and its mutants were grown in Bennet medium (35) at 30°C. *Sarcina lutea* was used as an indicator for rifamycin production (29). When needed, apramycin (50 μg/ml), kanamycin (50 μg/ml), and ampicillin (100 μg/ml) were used. Plasmids used in this study are listed in Table 2, and primers (ordered from Biosune [Shanghai]) are listed in Table S1 in the supplemental material. The DL1000 DNA ladder was ordered from TaKaRa.

Screening of the transposon mutants of *A. mediterranei* U32. Competent cells for electroporation were prepared according to our previous work (36). Electroporation of *A. mediterranei* U32 with methylation-free Tn*316* was carried out with the Gene Pulser apparatus (Bio-Rad). Specifically, 1 μg DNA was added into 60 μl U32 competent cells and mixed on ice, and the mixture was transferred to a chilled electroporation cuvette (2 mm). The field strength was 9 kV/cm, and the pulse duration was about 13 to 14 ms. After pulsing, 1 ml prewarmed Bennet medium was immediately added to the electroporation cuvette and the mixture was incubated at 30°C for 4 h. Then, the cells were plated on Bennet plates containing apramycin (50 μg/ml) to select out successfully transposed mutants. Proper-size colonies were arrayed into 96-well plates, where each well contained 100 μl 20% glycerol. Finally, these plates were frozen and stored at −80°C.

To screen rifamycin-deficient mutants, frozen mutants were plated onto Bennet plates and further incubated at 30°C for 4 days. Candidate mutants were inoculated into 50 ml liquid Bennet medium

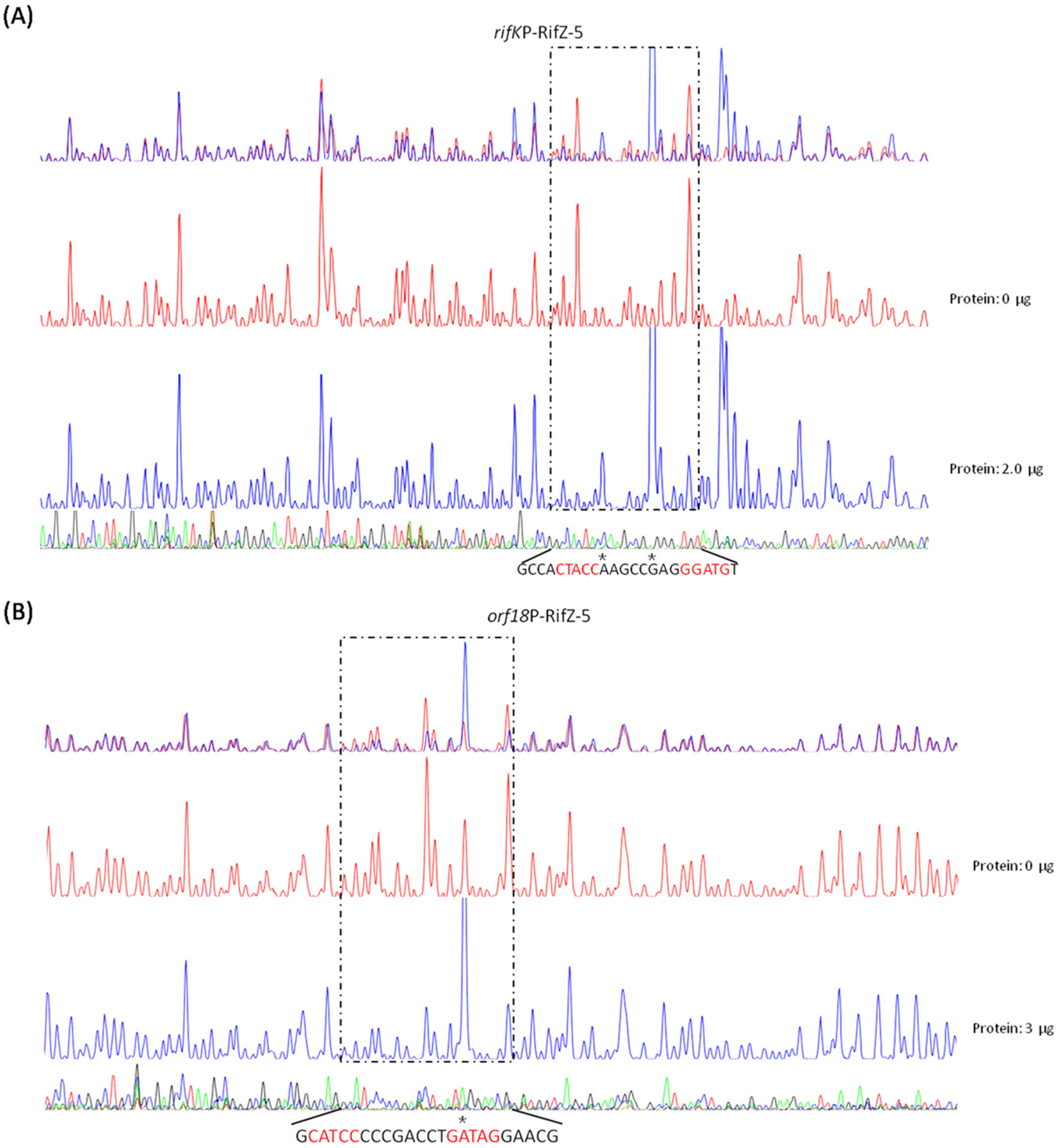

FIG 5 Verification of the binding of RifZ-5 to the promoter regions of *rifK* and *orf18* by DNase I footprinting assay. *rifK* (A) and *orf18* (B) were identified through searching with the RifZ box in U32 at the whole-genome scale. The DNase I footprinting assay further confirmed that RifZ could specifically bind to both promoter regions, and the two RifZ-5-protected DNA sequences contained the RifZ binding motif, which is highlighted in red.

and incubated at 30°C for 48 h with shaking at 200 rpm. Then, 2.5 ml culture was further inoculated into 50 ml fresh liquid Bennet medium, followed by continuing incubation for 22 h at 30°C with shaking at 200 rpm.

S. lutea was grown in 10 ml Luria-Bertani (LB) medium and incubated at 37°C for 18 h with shaking at 200 rpm. Then, the culture was mixed with 40 ml LB medium containing 0.8% low-melting agar and then poured onto LB plates containing 1.5% agar. Five microliters of supernatants of mutant cultures (22 h) was added to double plates with *S. lutea*, which were incubated at 37°C for phenotype observation. Growth of *S. lutea* was inhibited if the supernatant contained rifamycin.

TABLE 2 Plasmids used in this study

Plasmid name	Relevant characteristics	Source
Tn*316*	Plasmid derived from IS-204 in *Nocardia asteroides* YP21	Lab stock
pFDZ100	*E. coli-Streptomyces* shuttle vector, derivative obtained from pHZ1358, containing *attP0* site and *attB15* site, resistant to thiostrepton, ampicillin, and chloromycetin	Lab stock
pFDZ101	Derivative obtained from pMD19-T, containing *attB0* site and *attP6* site, resistant to ampicillin and apramycin	Lab stock
pTA0613	Derivative obtained from pMD19-T, containing *attB6* site and *attP13* site, resistant to ampicillin and apramycin	Lab stock
pFDZ103	Derivative obtained from pMD19-T, containing *attB13* site, *attP15* site, and *attP0* site, resistant to ampicillin and apramycin	Lab stock
pDZL101	Derivative obtained from pFDZ101, containing the upstream homologous arm of *AMED_0655*	This work
pDZL103	Derivative obtained from pFDZ103, containing the downstream homologous arm of *AMED_0655*	This work
pDZL104	Derivative obtained from pFDZ100, containing both homologous arms of *AMED_0655*, resistant to thiostrepton and apramycin	This work
pRT801	*E. coli-Streptomyces* shuttle plasmid, encoding the ϕBT1-integrase and containing *attP*, resistant to apramycin	40
pMD19-hyg	A 1,415-bp hygromycin resistance fragment flanked by two EcoRV sites in pMD19	Lab stock
pDZL803	EcoRV-digested fragment (1,409 bp) from pMD19-hyg ligated into the SmaI site of pRT801, resistant to apramycin and hygromycin	This work
pDZL8031	*AMED_0655* gene with its intact promoter ligated into the EcoRV site of pDZL803	This work
pET-RifZ1	*AMED_0655* gene ligated into pET28a(+)	This work
pET-RifZ5	Coding DNA sequence of RifZ-5 ligated into pET28a(+)	This work

Characterization of the transposon insertional sites in mutants. Genomic DNA was extracted using commercial genomic extraction kits and digested with FastDigest ApaI (Thermo Fisher Scientific) for about 3 h. After inactivation of ApaI, the digested mixture was ligated with T4 DNA ligase (Tolo Biotech, Shanghai, China) overnight before being transformed into competent cells of *E. coli* DH5α. Transformants selected on LB plates containing apramycin (50 μg/ml) were inoculated into 3 ml liquid LB medium and incubated overnight. Rescued plasmids were extracted and sequenced using primer MY-002, and sequences downstream of GAAGAGCC were rescued from the mutant genome. Assisted with alignment analysis, sites and directions of the transposon insertion were determined.

Construction of *rifZ* knockout mutant and its complementation strain. To knock out *rifZ via* homologous recombination, plasmids were constructed as previously described (37). Briefly, primers 0655U-F/0655U-R and 0655D-F/0655D-R were separately used to amplify the upstream and downstream homologous arms of *rifZ*, and the PCR fragments were introduced into the XcmI site of pFDZ101 and pFDZ103 to obtain pDZL101 and pDZL103 (Table 2), respectively. pDZL101, pDZL103, and pTA0613 were linearized and tandemly assembled with pFDZ100 using φBT1 integrase (38) to produce the knockout plasmid pDZL104, which was further electroporated into U32 to knock out *rifZ*. Mutants were selected on Bennet plates containing apramycin (50 μg/ml) and verified by PCR employing primers 0655CH-UF/0655CH-UR and 0655CH-DF/0655CH-DR.

The hygromycin resistance cassette from pMD19-hyg was inserted into the SmaI site of pRT801 (39, 40) to obtain plasmid pDZL803. The *rifZ* gene with its intact promoter region was amplified with primers 0655C-F/0655C-R using Phanta super-fidelity DNA polymerase (Vazyme) and inserted into the EcoRV site of pDZL803, producing plasmid pDZL8031. Plasmid pDZL8031 and the control plasmid pDZL803 were individually introduced into the *rifZ* null mutant by electroporation, obtaining both the complementation strain and its blank control.

RNA extraction and RT-PCR analysis. *A. mediterranei* strains were grown in liquid Bennet medium at 30°C for 48 h with shaking at 200 rpm, and then 2.5 ml culture was inoculated into 50 ml fresh liquid Bennet medium and further incubated for 22 h. Total RNA was extracted using TRIzol reagent (Thermo Fisher Scientific) and further treated with RNase-free DNase I (TaKaRa) to prevent contamination of trace genomic DNA. RT was performed using the PrimeScript II 1st Strand cDNA synthesis kit (TaKaRa). Then, PCR was performed with 20 ng cDNA as the template for 28 cycles, using the *rpoB* gene as the internal control. A negative control was made by following the same procedures except for the omission of reverse transcriptase during RT. Two independent samples were employed for analyses.

Cotranscription assay of all the genes in the *rif* cluster of *A. mediterranei* U32. After being cultured at 30°C in Bennet medium containing 80 mM KNO_3 for 24 h, cells were harvested and used to extract total RNA, which was then used for cDNA synthesis. With the cDNA as the template, cotranscription assay of genes (from *rifT* to *rifZ*) was achieved by PCR. At the same time, the negative and positive controls were achieved by PCRs with the total RNA and genomic DNA (gDNA) of *A. mediterranei* U32 as the templates separately. Primers used during PCRs are listed in Table S1. The principle for designing the cotranscription assay primers was as follows: the forward primer was designed at the end of one gene, while the reverse primer was located at the middle of the next gene.

Protein expression in *E. coli* BL21(DE3). The amino acid sequence of RifZ was analyzed on NCBI, and the DNA binding domain of RifZ (namely RifZ-5) was predicted to be from aa 346 to 398. To construct plasmids expressing complete and truncated RifZ proteins, the coding DNA sequence was amplified with different primer pairs (from RifZ-1EX-F/RifZ-EX-R to RifZ-5EX-F/RifZ-EX-R [see Fig. S1 in the supplemental material]). PCR amplicons were digested with NdeI and HindIII, and then they were introduced into the same sites in pET-28a(+), generating the expression plasmids pET-RifZ1 to pET-RifZ5.

The expression plasmids were then transformed into *E. coli* BL21(DE3), and induction of the protein expression was performed by addition of 0.2 mM IPTG (isopropyl-β-D-thiogalactopyranoside) and grown

at 16°C for 16 h. Cells were harvested, washed twice in potassium phosphate buffer (pH 7.0), and lysed using an ultrasonic cell crusher. In noninduced samples, cells were directly treated with the BugBuster master mix (Novagen) before being loaded for sodium dodecyl sulfate-polyacrylamide gel electrophoresis (SDS-PAGE) analysis. To prevent protein degradation, 1 mM (final concentration) phenylmethylsulfonyl fluoride (PMSF) was added. After separation of the cell debris and membrane fractions from the soluble fraction by centrifugation at 15,000 rpm for 30 min using a high-speed refrigerated centrifuge (CR21GIII; Hitachi), His-tagged full-length and truncated RifZ proteins were purified by Ni-nitrilotriacetic acid (Ni-NTA) gravity flow columns and further assessed by SDS-PAGE. Protein concentrations were determined by the Bradford method (41).

Electrophoretic mobility shift assay and DNase I footprinting assay. Promoter regions were amplified by PCR with Dpx DNA polymerase (Tolo Biotech, Shanghai, China), employing the primer pairs listed in Table S1. Purified PCR amplicons were separately cloned into the TA cloning vector pUC18B-T (Tolo Biotech) and verified through DNA sequencing. Then, plasmids were used as the templates for probe preparation by PCR using primers M13F-47 (FAM labeled) and M13R-48. FAM-labeled probes were purified using Wizard SV gel and the PCR Clean-Up system (Promega) and quantified with a NanoDrop 2000C spectrophotometer (Thermo Fisher Scientific).

The binding of RifZ-5 to probes was carried out in a 20-μl reaction volume containing 50 mM Tris-HCl (pH 8.0), 100 mM KCl, 2.5 mM $MgCl_2$, 1.0 mM dithiothreitol (DTT), 10% glycerol, and 100 ng/μl sheared salmon sperm DNA. FAM-labeled probes (40 ng) and different amounts (0 and 2 μg) of His-tagged RifZ-5 were used for each reaction. After being incubated for 30 min at 30°C, samples were separated by a 6% native polyacrylamide gel in ice-bathed 0.5× Tris-borate-EDTA (TBE) at 150 V. Gels were scanned with an ImageQuant LAS 4000mini imager (GE Healthcare).

DNase I footprinting assays were performed by Tolo Biotech according to the procedures previously described (18). In brief, about 400 ng FAM-labeled probes was incubated with different amounts of His-tagged RifZ-5 in a total volume of 40 μl. After incubation, DNase I digestion was performed for 1 min at room temperature before being stopped by addition of the DNase I stop solution. Digested samples were purified and then loaded into an ABI 3130 sequencer for electrophoresis. The electropherograms were analyzed with PeakScanner v1.0 software (Applied Biosystems).

SUPPLEMENTAL MATERIAL

Supplemental material for this article may be found at https://doi.org/10.1128/AEM.03201-16.

SUPPLEMENTAL FILE 1, PDF file, 1.7 MB.

ACKNOWLEDGMENTS

This work was supported by grants from the National Key Research Development Program of China (2016YFA0500600), the National Natural Science Foundation of China (no. 31430004, 31670058, and 31300034), and the China National Basic Research Program (973 Program no. 2012CB721102).

We thank Tolo Biotech for their assistance in protein purification, EMSA, and DNase I footprinting assay. We thank Shuangxi Ren for his help in bioinformatics analysis.

REFERENCES

1. Calvori C, Frontali L, Leoni L, Tecce G. 1965. Effect of rifamycin on protein synthesis. Nature 207:417–418. https://doi.org/10.1038/207417a0.
2. Atre SR, Murray MB. 2016. Management and control of multidrug-resistant tuberculosis (MDR-TB): addressing policy needs for India. J Public Health Policy https://doi.org/10.1057/jphp.2016.14.
3. Velayati AA, Farnia P, Masjedi MR. 2013. Totally drug-resistant tuberculosis (TDR-TB): a debate on global health communities. Int J Mycobacteriol 2:71–72. https://doi.org/10.1016/j.ijmyco.2013.04.005.
4. Wehrli W, Knusel F, Schmid K, Staehelin M. 1968. Interaction of rifamycin with bacterial RNA polymerase. Proc Natl Acad Sci U S A 61:667–673. https://doi.org/10.1073/pnas.61.2.667.
5. Campbell EA, Korzheva N, Mustaev A, Murakami K, Nair S, Goldfarb A, Darst SA. 2001. Structural mechanism for rifampicin inhibition of bacterial RNA polymerase. Cell 104:901–912. https://doi.org/10.1016/S0092-8674(01)00286-0.
6. August PR, Tang L, Yoon YJ, Ning S, Muller R, Yu TW, Taylor M, Hoffmann D, Kim CG, Zhang X, Hutchinson CR, Floss HG. 1998. Biosynthesis of the ansamycin antibiotic rifamycin: deductions from the molecular analysis of the rif biosynthetic gene cluster of Amycolatopsis mediterranei S699. Chem Biol 5:69–79. https://doi.org/10.1016/S1074-5521(98)90141-7.
7. Tang B, Zhao W, Zheng H, Zhuo Y, Zhang L, Zhao GP. 2012. Complete genome sequence of Amycolatopsis mediterranei S699 based on de novo assembly via a combinatorial sequencing strategy. J Bacteriol 194:5699–5700. https://doi.org/10.1128/JB.01295-12.
8. Verma M, Kaur J, Kumar M, Kumari K, Saxena A, Anand S, Nigam A, Ravi V, Raghuvanshi S, Khurana P, Tyagi AK, Khurana JP, Lal R. 2011. Whole genome sequence of the rifamycin B-producing strain Amycolatopsis mediterranei S699. J Bacteriol 193:5562–5563. https://doi.org/10.1128/JB.05819-11.
9. Zhao W, Zhong Y, Yuan H, Wang J, Zheng H, Wang Y, Cen X, Xu F, Bai J, Han X, Lu G, Zhu Y, Shao Z, Yan H, Li C, Peng N, Zhang Z, Zhang Y, Lin W, Fan Y, Qin Z, Hu Y, Zhu B, Wang S, Ding X, Zhao GP. 2010. Complete genome sequence of the rifamycin SV-producing Amycolatopsis mediterranei U32 revealed its genetic characteristics in phylogeny and metabolism. Cell Res 20:1096–1108. https://doi.org/10.1038/cr.2010.87.
10. Absalon AE, Fernandez FJ, Olivares PX, Barrios-Gonzalez J, Campos C, Mejia A. 2007. RifP; a membrane protein involved in rifamycin export in Amycolatopsis mediterranei. Biotechnol Lett 29:951–958. https://doi.org/10.1007/s10529-007-9340-7.
11. Floss HG, Yu TW. 1999. Lessons from the rifamycin biosynthetic gene cluster. Curr Opin Chem Biol 3:592–597. https://doi.org/10.1016/S1367-5931(99)00014-9.
12. Kaur H, Cortes J, Leadlay P, Lal R. 2001. Cloning and partial characterization of the putative rifamycin biosynthetic gene cluster from the actinomycete Amycolatopsis mediterranei DSM 46095. Microbiol Res 156:239–246. https://doi.org/10.1078/0944-5013-00108.
13. Schupp T, Toupet C, Engel N, Goff S. 1998. Cloning and sequence analysis of the putative rifamycin polyketide synthase gene cluster from

Amycolatopsis mediterranei. FEMS Microbiol Lett 159:201–207. https://doi.org/10.1111/j.1574-6968.1998.tb12861.x.
14. Yuan H, Zhao W, Zhong Y, Wang J, Qin Z, Ding X, Zhao GP. 2011. Two genes, rif15 and rif16, of the rifamycin biosynthetic gene cluster in Amycolatopsis mediterranei likely encode a transketolase and a P450 monooxygenase, respectively, both essential for the conversion of rifamycin SV into B. Acta Biochim Biophys Sin (Shanghai) 43:948–956. https://doi.org/10.1093/abbs/gmr091.
15. Rodriguez-Garcia A, Sola-Landa A, Apel K, Santos-Beneit F, Martin JF. 2009. Phosphate control over nitrogen metabolism in Streptomyces coelicolor: direct and indirect negative control of glnR, glnA, glnII and amtB expression by the response regulator PhoP. Nucleic Acids Res 37:3230–3242. https://doi.org/10.1093/nar/gkp162.
16. Sola-Landa A, Rodriguez-Garcia A, Amin R, Wohlleben W, Martin JF. 2013. Competition between the GlnR and PhoP regulators for the glnA and amtB promoters in Streptomyces coelicolor. Nucleic Acids Res 41:1767–1782. https://doi.org/10.1093/nar/gks1203.
17. Wang J, Zhao GP. 2009. GlnR positively regulates nasA transcription in Streptomyces coelicolor. Biochem Biophys Res Commun 386:77–81. https://doi.org/10.1016/j.bbrc.2009.05.147.
18. Wang Y, Cen XF, Zhao GP, Wang J. 2012. Characterization of a new GlnR binding box in the promoter of amtB in Streptomyces coelicolor inferred a PhoP/GlnR competitive binding mechanism for transcriptional regulation of amtB. J Bacteriol 194:5237–5244. https://doi.org/10.1128/JB.00989-12.
19. Wang Y, Wang JZ, Shao ZH, Yuan H, Lu YH, Jiang WH, Zhao GP, Wang J. 2013. Three of four GlnR binding sites are essential for GlnR-mediated activation of transcription of the Amycolatopsis mediterranei nas operon. J Bacteriol 195:2595–2602. https://doi.org/10.1128/JB.00182-13.
20. Kitani S, Ikeda H, Sakamoto T, Noguchi S, Nihira T. 2009. Characterization of a regulatory gene, aveR, for the biosynthesis of avermectin in Streptomyces avermitilis. Appl Microbiol Biotechnol 82:1089–1096. https://doi.org/10.1007/s00253-008-1850-2.
21. Wilson DJ, Xue Y, Reynolds KA, Sherman DH. 2001. Characterization and analysis of the pikD regulatory factor in the pikromycin biosynthetic pathway of Streptomyces venezuelae. J Bacteriol 183:3468–3475. https://doi.org/10.1128/JB.183.11.3468-3475.2001.
22. Aparicio JF, Molnár I, Schwecke T, König A, Haydock SF, Khaw LE, Staunton J, Leadlay PF. 1996. Organization of the biosynthetic gene cluster for rapamycin in Streptomyces hygroscopicus: analysis of the enzymatic domains in the modular polyketide synthase. Gene 169:9–16. https://doi.org/10.1016/0378-1119(95)00800-4.
23. He W, Lei J, Liu Y, Wang Y. 2008. The LuxR family members GdmRI and GdmRII are positive regulators of geldanamycin biosynthesis in Streptomyces hygroscopicus 17997. Arch Microbiol 189:501–510. https://doi.org/10.1007/s00203-007-0346-2.
24. Rascher A, Hu Z, Viswanathan N, Schirmer A, Reid R, Nierman WC, Lewis M, Hutchinson CR. 2003. Cloning and characterization of a gene cluster for geldanamycin production in Streptomyces hygroscopicus NRRL. 3602. FEMS Microbiol Lett 218:223–230. https://doi.org/10.1016/S0378-1097(02)01148-5.
25. Zhu Z, Li H, Yu P, Guo Y, Luo S, Chen Z, Mao X, Guan W, Li Y. 2016. SlnR is a positive pathway-specific regulator for salinomycin biosynthesis in Streptomyces albus. Appl Microbiol Biotechnol https://doi.org/10.1007/s00253-016-7918-5.
26. Lo Grasso L, Maffioli S, Sosio M, Bibb M, Puglia AM, Alduina R. 2015. Two master switch regulators trigger A40926 biosynthesis in Nonomuraea sp. strain ATCC 39727. J Bacteriol 197:2536–2544.
27. Horbal L, Kobylyanskyy A, Truman AW, Zaburranyi N, Ostash B, Luzhetskyy A, Marinelli F, Fedorenko V. 2014. The pathway-specific regulatory genes, tei15* and tei16*, are the master switches of teicoplanin production in Actinoplanes teichomyceticus. Appl Microbiol Biotechnol 98:9295–9309. https://doi.org/10.1007/s00253-014-5969-z.
28. Schaefer AL, Hanzelka BL, Eberhard A, Greenberg EP. 1996. Quorum sensing in Vibrio fischeri: probing autoinducer-LuxR interactions with autoinducer analogs. J Bacteriol 178:2897–2901. https://doi.org/10.1128/jb.178.10.2897-2901.1996.
29. Yu H, Yao Y, Liu Y, Jiao R, Jiang W, Zhao GP. 2007. A complex role of Amycolatopsis mediterranei GlnR in nitrogen metabolism and related antibiotics production. Arch Microbiol 188:89–96. https://doi.org/10.1007/s00203-007-0228-7.
30. Yao W, Yang Y, Chiao J. 1994. IS204: an insertion sequence from Nocardia asteroides (mexicana) YP21. Plasmid 32:262–269. https://doi.org/10.1006/plas.1994.1065.
31. Zhang X, Bao Y, Shi X, Ou X, Zhou P, Ding X. 2012. Efficient transposition of IS204-derived plasmids in Streptomyces coelicolor. J Microbiol Methods 88:67–72. https://doi.org/10.1016/j.mimet.2011.10.018.
32. Ou X, Zhang B, Zhang L, Dong K, Liu C, Zhao G, Ding X. 2008. SarA influences the sporulation and secondary metabolism in Streptomyces coelicolor M145. Acta Biochim Biophys Sin (Shanghai) 40:877–882. https://doi.org/10.1111/j.1745-7270.2008.00466.x.
33. Ou X, Zhang B, Zhang L, Zhao G, Ding X. 2009. Characterization of rrdA, a TetR family protein gene involved in the regulation of secondary metabolism in Streptomyces coelicolor. Appl Environ Microbiol 75:2158–2165. https://doi.org/10.1128/AEM.02209-08.
34. Shao ZH, Ren SX, Liu XQ, Xu J, Yan H, Zhao GP, Wang J. 2015. A preliminary study of the mechanism of nitrate-stimulated remarkable increase of rifamycin production in Amycolatopsis mediterranei U32 by RNA-seq. Microb Cell Fact 14:75. https://doi.org/10.1186/s12934-015-0264-y.
35. Mejia A, Barrios-Gonzalez J, Viniegra-Gonzalez G. 1998. Overproduction of rifamycin B by Amycolatopsis mediterranei and its relationship with the toxic effect of barbital on growth. J Antibiot (Tokyo) 51:58–63. https://doi.org/10.7164/antibiotics.51.58.
36. Ding X, Tian Y, Chiao J, Zhao G, Jiang W. 2003. Stability of plasmid pA387 derivatives in Amycolatopsis mediterranei producing rifamycin. Biotechnol Lett 25:1647–1652. https://doi.org/10.1023/A:1025698824679.
37. Zhang B, Zhang L, Dai R, Yu M, Zhao G, Ding X. 2013. An efficient procedure for marker-free mutagenesis of S. coelicolor by site-specific recombination for secondary metabolite overproduction. PLoS One 8:e55906. https://doi.org/10.1371/journal.pone.0055906.
38. Zhang L, Ou X, Zhao G, Ding X. 2008. Highly efficient in vitro site-specific recombination system based on streptomyces phage phiBT1 integrase. J Bacteriol 190:6392–6397. https://doi.org/10.1128/JB.00777-08.
39. Baltz RH. 2012. Streptomyces temperate bacteriophage integration systems for stable genetic engineering of actinomycetes (and other organisms). J Ind Microbiol Biotechnol 39:661–672. https://doi.org/10.1007/s10295-011-1069-6.
40. Gregory MA, Till R, Smith MC. 2003. Integration site for Streptomyces phage phiBT1 and development of site-specific integrating vectors. J Bacteriol 185:5320–5323. https://doi.org/10.1128/JB.185.17.5320-5323.2003.
41. Bradford MM. 1976. A rapid and sensitive method for the quantitation of microgram quantities of protein utilizing the principle of protein-dye binding. Anal Biochem 72:248–254. https://doi.org/10.1016/0003-2697(76)90527-3.